Scanning Coherent Diffraction Imaging (Ptychography)

Janet S. Lee

October 30, 2018

Abstract

The traditional method of coherent diffraction imaging requires a single diffraction pattern to be taken with varying exposure times at a fixed position. By averaging among these images we can use a reiterative phase retrieval algorithm to reconstruct our sample. Ptychography is advantageous to regular CDI because it allows us to cover an extended area of the sample by moving it around on a mount and taking different diffraction patterns. The edge of a bee wing and roughly half of a UCLA metal mask were reconstruction in this experiment. The metal mask was moved at 96 μm increments and images were taken at five different exposure times. In future applications of ptychography we will be taking a greater number of images at each exposure time, increasing the overlap between adjacent positions and sampling a greater area on the sample.

1 Introduction

Light microscopy employs light to magnify an object, often a biological sample. Specifically, bright field microscopy is used in this experiment which is when the sample is placed in between the light source and the detector. The light passing through the sample creates a diffraction image, which is then sent through a lens. With a detector placed at the focal point downstream of the lens, we can capture the information in phase space.

1.1 Coherent Diffraction Imaging(CDI)

CDI involves shooting a laser at a sample followed by a lens and detector. The "Cohesive" part comes from the requirement that the light source be both spatially and temporally cohesive, meaning that it should have a fixed relative phase, ensuring that the resulting amplitudes and phases are not arbitrary and that the interference will create a meaningful diffraction pattern. The path lengths required for both are expressed in the following equations:

$$l_{spatial} = \frac{x\lambda}{2\pi d}$$

$$l_{temporal} = \frac{\lambda^2}{2\Delta\lambda}$$

The "Diffraction" component is important because the images that are taken and reconstructed are the diffraction patterns from the sample. Given that the set up is aligned such that the beam is pointed straight at the sample and that every component on the workbench is centered correctly, the resulting diffraction pattern should be centro-symmetric. Centro-symmetry will result with any sample because considering a real object, $g(x)$, the diffraction intensity is proportional to the square of the Fourier transform, $|G(f)|^2$, and we can prove that $|G(f)|^2 = |G(-f)|^2$ as follows:

$$G(f) = \int_{-\infty}^{\infty} g(x)\, e^{-2\pi i f x} dx$$

$$G(-f) = \int_{-\infty}^{\infty} g(x)\, e^{2\pi i f x} dx$$

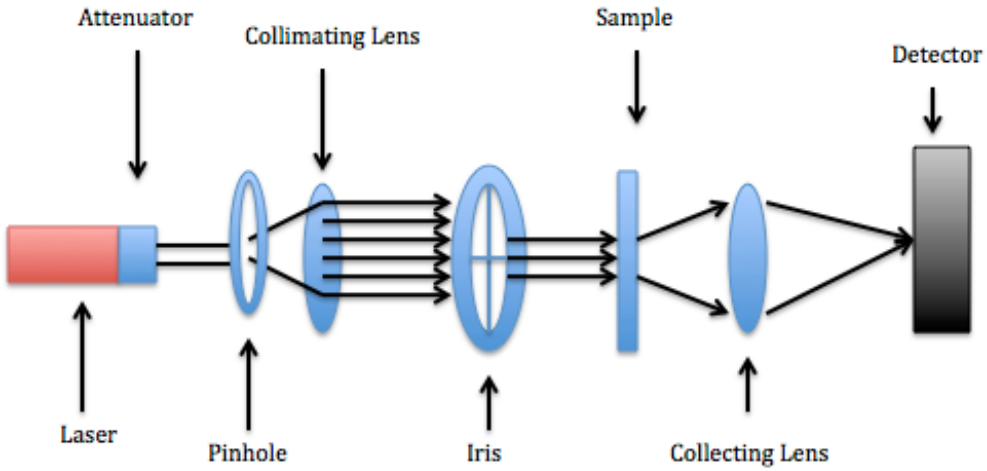

Figure 1: The figure above shows the set up for our experiment. The distance between the first pinhole and the collimating lens was its focal length, 50 mm, and the distance between the collecting lens and the detector was 100 mm so that it would detect the diffraction image in phase space.

$$G^*(-f) = \int_{-\infty}^{\infty} g^*\ e^{-2\pi i f x} dx$$
$$= \int_{-\infty}^{\infty} g(x)\ e^{-2\pi i f x} dx$$
$$G^*(-f) = G(f)$$
$$|G(f)|^2 = |G(-f)|^2$$

Thus for any real object, $g(x)$, we can expect to see centro-symmetric diffraction patterns.

Additionally a collimation system is necessary to ensure a plane wave illumination on the sample. This system consists of a pinhole to create a point source of light, a lens to create Fraunhofer diffraction, and an iris to only have the central beam on the sample.

Lastly a python program is used to retrieve the phase information of the diffraction pattern. This is necessary because there are two components to a wave: its amplitude and phase. The detector gathers the intensity information, which is proportional to the modulus squared of the wave. As a result, the phase information of the wave disappears because of its complex nature. The phase retrieval algorithm used was the Hybrid Input Output.

1.2 Hybrid Input Output (HIO)

The image that we detect is in phase space because the detector is placed at the focal point of the collecting lens. This program solves the phase problem by applying a random phase to the detected image, $G(f)$, and then applying an inverse Fourier transform to bring it back to real space. Then the error is reduced, by the system shown below:

$$g_2(\vec{r}) = \begin{cases} 0 & \text{if } \vec{r} \notin S) \cup [g_1(\vec{r}) < 0] \\ g_1(\vec{r}) & \text{Otherwise} \end{cases}$$

For HIO, the following system is used for reconstruction:

$$g_2(\vec{r}) = \begin{cases} g_1(\vec{r}) - \beta g_1(\vec{r}) & \text{if } \vec{r} \notin S) \cup [g_1(\vec{r}) < 0] \\ g_1(\vec{r}) & \text{Otherwise} \end{cases}$$

Figure 2: The figure above shows our workbench with everything screwed in.

Once this is done, the Fourier Transform is applied, and the process is repeated until error is minimized. The program stops when the error is at the minimum and we are given a magnified image of the sample from the diffraction pattern.

1.3 Ptychography

Regular CDI is done on a stationary sample and images with a single diffraction pattern by the process described above. Ptychography, scanning CDI, is when the sample is moved to varying positions, which are measured and recorded, and the diffraction patterns of multiple images are used in reconstruction. From position to position, we allow for at least 50% overlap. The greater the overlap, the better the reconstruction is because the same section of the sample is taken into consideration in the reiterative algorithm. Additionally, adjustments are made to the reiterative algorithm because the positions of the sample need to be recorded to create the correct reconstruction. Another difference in the program was that since we added a pinhole in front of the sample, the resulting image was a convolution of a probe function and the sample. We needed to guess the probe function and deconvolve the two. This is possible because of the useful fact that the Fourier transform of two convolved functions is equal to the product of the Fourier transform of the individual functions. For two functions $g(x)$ and $h(x)$ with Fourier transforms $G(x)$ and $H(x)$ respectively, $G(x)H(x)$ is equivalent to the Fourier transform of $g(x) \otimes h(x)$.

2 Experimental Method

A 635 nm laser was placed at the edge of the board and attenuators of varying strengths were used to keep the CCD (charge-coupled device) from being over-saturated. Downstream from the attenuator we set up our collimation system as described in the introduction. A 50 μm pinhole was used with a 50 mm plano convex lens. Then an iris was placed after the lens so that we could adjust the modes that passed through it. Downstream from the iris we placed another pinhole of size 100 μm before our sample, then added a collecting lens with a 150 mm focal length before the detector.

We initially used a bee wing as our biological sample and it was placed between two thin glass slides to keep it in place. The slides were then secured onto a movable mount with two degrees of freedom. There were two knobs to indicate the amount we were changing the position. Each tick on the knob moved the mount by 24 μm. We first used this set up to get a single diffraction

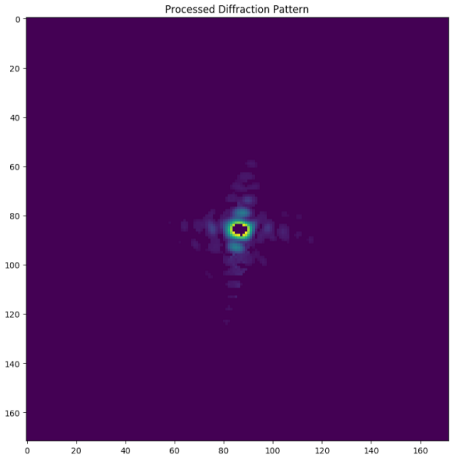

Figure 3: The image above is the diffraction pattern we used to reconstruct our image of the bee wing. The cross-like pattern we see is from the mask we used on the sample.

pattern and test the HIO program. To get a clearer diffraction pattern, we took out the glass slides and instead glued the wing onto the edge of the mount so that the beam would directly hit the sample. This later proved to be a problem because although the sample was transparent enough that the beam would go through, the wing was not completely flat which kept us from finding centro-symmetric diffraction patterns, and the wing decayed too quickly for us to get consistent data throughout the weeks.

As a result, the bee wing was switched out for a metal mask with the UCLA logo cut out at the center. By taping the mask onto a post and placing a 100 μm pinhole as close to the sample as possible to get a point source for the light, we collected the diffraction patterns of the mask at nine different positions. The positions formed a three by three square on the mask and each square had dimensions of 96 μm x 96 μm. Before starting to take these measurements we had to go through each position and make sure we were getting centro-symmetric diffraction patterns for each position. In addition, the iris was taken out for this step because we had the second pinhole that would cut out the extra modes.

Images were taken at five different exposure times so that we could average over them. We started at a time where the central beam was almost saturated and increased the exposure time at 0.1 second increments until the saturated central beam started bleeding into the first diffraction mode. At the highest exposure time, when the diffraction patterns were the clearest, we took four extra images so that we could average the patterns and get a better reconstruction.

3 Experimental Results and Discussion

For the first part of the experiment we took the bee wing as a sample. After carefully mounting the wing between two thin glass slides and shooting the laser at a curved edge of the wing, we were able to recover an image from single diffraction. Figure 3 shows the diffraction pattern used and Figure 4 shows the reconstructed image. Because we only used one diffraction pattern to first test the program, the reconstruction has poor resolution and it is difficult to make out the details of the wing. However, we can see the clear edge of the wing because we do not see any pattern on the left side of the reconstructed image.

After deciding that the bee wing was not going to give us usable diffraction patterns and that its decay rate made it difficult to gather consistent data, we switched out the sample. We instead used a metal mask with the UCLA logo cut out of it at the center. We also switched out the 100 μm pinhole for a 200 μm pinhole to get a bigger beam size and thus increase the overlap between adjacent positions. By mounting this on a post and placing it on our movable mount, we

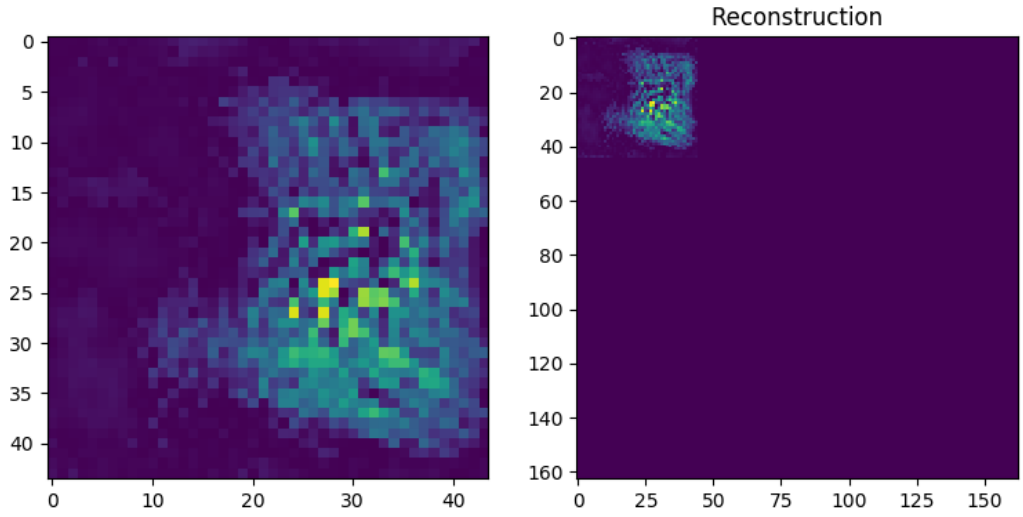

Figure 4: The reconstruction shows the edge of the bee wing that was reconstructed from one diffraction image. The sample was placed between two glass slides and the laser was positioned to hit the edge of the wing.

were able to get better diffraction patterns. Before performing ptychography on this sample, we took another single diffraction pattern (shown in Figure 5) and reconstructed it as a test run. The reconstruction in Figure 6 shows a clear "U" of the "UCLA."

Once we ensured the diffraction pattern could give us accurate reconstructions, we began performing scanning CDI (ptychography) by starting at the top left corner of our 3 x 3 position grid. By moving the knobs at 96 μm increments in the x and y directions, we were able to cover the nine positions while maintaining at roughly 50% overlap between them. As explained in the Methods section, we took images at five different exposure times, taking an extra four images at the highest exposure time. Using a text file to record the positions, we ran the iterative algorithm for ptychography and found the reconstruction to be as shown in Figure 7.

This reconstruction is not as clear as the single diffraction used when reconstructing Figure 6 because we took less images of the diffraction patterns at each exposure in the interest of time. Ptychography proved to be a very time consuming process because once we found a usable, centrosymmetric pattern, we had to take multiple images at varying exposure times. This process was repeated for each of the nine positions. The pinhole was estimated to be a circular probe in the python program.

Furthermore, multiple realignments were necessary because as we put in our samples, we would realize that the laser and collimation system was not perfectly aligned. Ptychography was very unforgiving with misalignment, so another time consuming component of our experiment was aligning the beam.

4 Conclusion

Extended areas of both the bee wing and the UCLA mask were imaged using ptychography. Scanning CDI proved to be advantageous over regular CDI because of its ability to reconstruct greater areas of the sample and give clearer results because the overlapping regions provided more

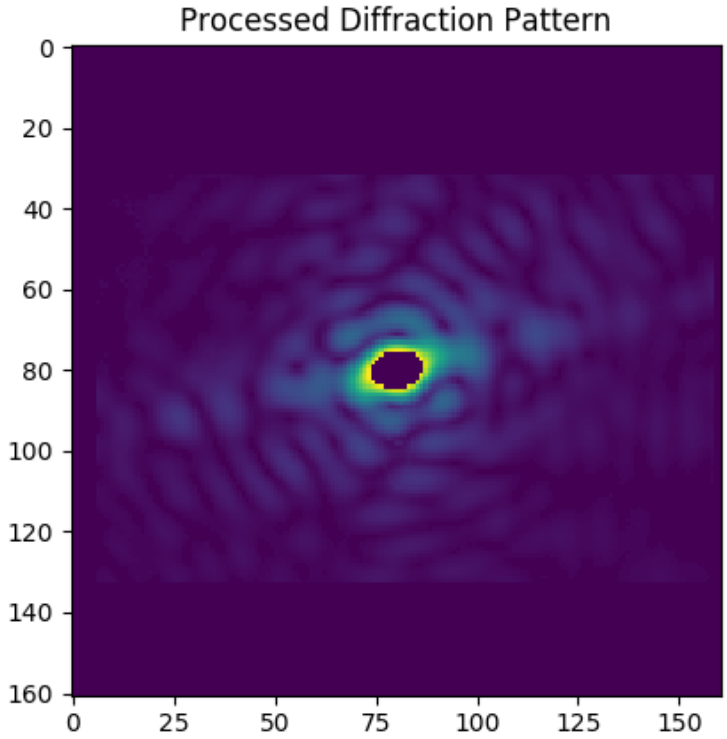

Figure 5: The image above shows the diffraction pattern obtained once we switched out the bee wing sample and put in a UCLA mask instead. We can see the centro-symmetry clearly in this pattern where the exposure time is set to the maximum time without the saturation bleeding into any of the modes.

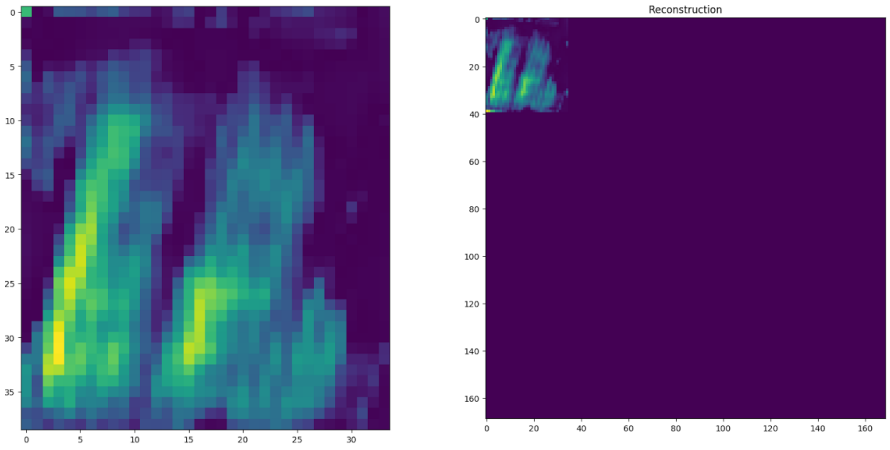

Figure 6: The set of images above shows the reconstruction from the UCLA mask. The cursive "U" is clearly visible.

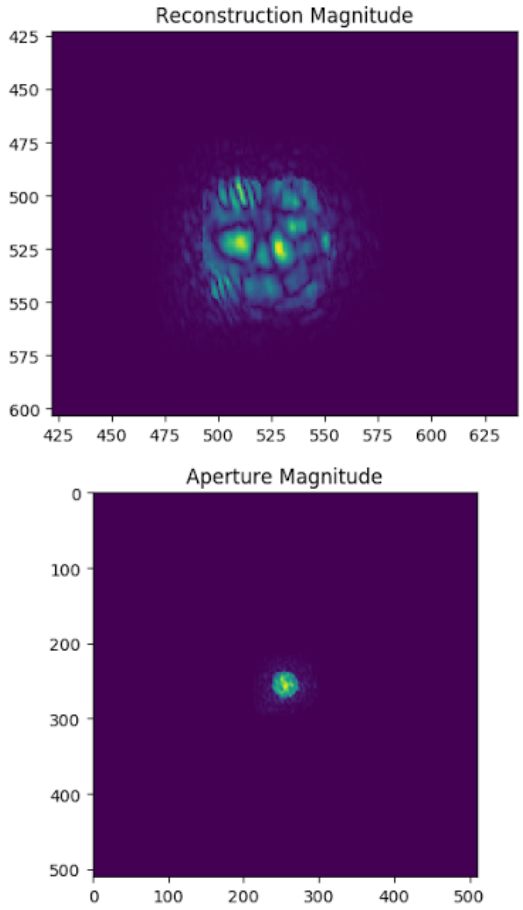

Figure 7: These images show the reconstruction of the diffraction patterns from the UCLA mask using ptychography.

data on the sample. Reconstruction with the single diffraction patterns in our experiment gave better results only because we had more images of those diffraction patterns. The limiting factor in our ptychography experiment was time because saving the images for each position at each exposure time took too long. Moreover, we could have improved our results had we increased the overlap by moving the knobs of the movable mount at smaller increments, and taken the position grid to be bigger in dimension.

4.1 Future Work

Manually moving the sample by turning the knobs was unreliable and led to a high source of error. The dimensions of the position grid were 96 μmx96 μm so a high level of accuracy was required to get a good reconstruction. A digital mount would be more precise in moving the sample. Furthermore, ptychography on a biological sample could be more applicable so long as the sample is completely flat and is preserved correctly so that centro-symmetric diffraction patterns and consistent data is achieved.

References

[1] Thibaulta P, Rankenburgb I, Optical diffraction microscopy in a teaching laboratory , (2007)

[2] Miao J, Charalambous P, Extending the methodology of X-ray crystallography to allow imaging of micrometre-sized non-crystalline specimens, (1990)

[3] Maiden A, Rodenburg J, optical ptychography: a practical implementation with useful resolution, (2010)